



Monoterpenoids isomerization and cyclization processes in Gewürztraminer wines: A kinetic investigation at different pH and temperatures

Panagiotis Arapitsas^{a,b}, Silvia Carlin^{a,*}, Fulvio Mattivi^a, Attilio Rapaccioli^c, Urska Vrhovsek^a, Graziano Guella^{d,*}

^a Research and Innovation Center, Fondazione Edmund Mach, 38010 San Michele all'Adige, Italy

^b Department of Wine, Vine, and Beverage Sciences, School of Food Science, University of West Attica, 12243 Athens, Greece

^c C3A, Center of Agriculture, Food and Environment, University of Trento, 38010 Trento, Italy

^d Bio-organic Chemistry Laboratory, Department of Physics, University of Trento, 38010 Trento, Italy

ARTICLE INFO

Keywords:

Terpenes
Reaction
Kinetic constant
Activation energy
Activation enthalpy
Activation entropy
Arrhenius plot
Eyring equation

ABSTRACT

The evolution of volatile compounds in wine comprises several acid-catalyzed reactions, such as glycosides precursors' hydrolysis and rearrangements, and significantly contributes to its sensory qualities, even after prolonged aging. The aim of this work was to use a well-defined experimental design and to examine how terpenoids in Gewürztraminer wine change over time when subjected to different temperatures and pH levels over two weeks. A theoretically-based approach was used, involving the definition of a complete system of ordinary differential equations (ODE) with well-established boundary conditions (initial concentration of reactants/products), using Kinetoscope, a kinetic simulation software. The calculated optimal rate constants, based on the experimental curves, produced a comprehensive data set describing the evolution of the terpenoid profile, highlighting the reversible and irreversible interconversion processes. Finding revealed that higher pH and lower temperature conditions are crucial for preserving the important terpenoid compounds that characterize the typicality and exemplarity of Gewürztraminer aroma profile.

1. Introduction

Aroma composition is a key element in explaining wines' quality, identity, and aging potential. However, aromatic wines produced from cultivars that have a high concentration of free and bound primary aroma compounds represent an ideal matrix to study the kinetics of terpenoid reactions. Gewürztraminer is not just a highly aromatic grape cultivar, rich in glycosides and free terpenes, but also produces worldwide premium wines of a wide pH range and aging potential (Lukić et al., 2016). Gewürztraminer wines are typically characterized by a scent of rose petals, cloves, lychees, and other tropical fruits. They are cultivated in 23 countries (12,823 ha worldwide), including Italy (1231 ha), where they are mainly found in the Trentino Alto Adige region (Ferretti & Febbroni, 2022). The wines of this variety have a variable aging potential and can be consumed both when young or aged, if stored properly. All these characteristics make Gewürztraminer wines an excellent model to study and understand the behavior of volatile

compounds during aging in a real matrix, under various conditions. Not all Gewürztraminer wines are made to be aged. However, those from the best vintages and vineyards can age for 8 years or more when stored in ideal conditions. An example of this effort towards taking storage to higher levels is the Epokale Gewürztraminer from Cantina Tramin in Alto-Adige, Italy, an ultra-premium white wine cellared at constant 11 °C for six years inside a disused silver mine at over 2000 m of altitude, claiming an ageing potential of over 20 years. Tramin's Epokale 2009 became the first Italian white wine to be awarded 100 points by Robert Parker's Wine Advocate in 2018. This wine, similarly to other premium quality Gewürztraminer in the Trentino-Alto Adige area, are characterized by a pH value around 3.7 which is common for red wines, while rather unusual in the panorama of internationally renowned whites.

Several studies have pointed out the richness of the Gewürztraminer grapes in primary aroma compounds, both in terms of quality and quantity, since they are characterized by a great concentration of monoterpenoids, such as linalool, geraniol, nerol and rose oxide

* Corresponding authors.

E-mail addresses: silvia.carlin@fmach.it (S. Carlin), graziano.guella@unitn.it (G. Guella).

<https://doi.org/10.1016/j.foodres.2024.115017>

Received 13 June 2024; Received in revised form 8 August 2024; Accepted 1 September 2024

Available online 15 September 2024

0963-9969/© 2024 The Author(s). Published by Elsevier Ltd. This is an open access article under the CC BY license (<http://creativecommons.org/licenses/by/4.0/>).

(Katarina et al., 2014; Lukić et al., 2016; Versini, 1985). Monoterpenoids are particularly abundant in aromatic grape cultivars, like Gewürztraminer, where they are present both in free form and multiple glycosides form (Gunata et al., 1985; Hjelmeland and Ebeler 2015). Among the aromatic grape varieties, Gewürztraminer is considered the richest in glycosylated monoterpenes, since the sum of the terpenes present in the wine, after enzymatic hydrolysis can exceed 4000 µg/L, while before hydrolysis their free form usually reach about 700–800 µg/L (Katarina et al., 2014; Ugliano & Moio, 2008; Versini, 1985). These non-volatile glycosides are defined as potential aromatic precursors, because during fermentation or storage they can be hydrolyzed either via enzymatic or acid catalysed mode and release the free aglycones. The *cis* isomer of rose oxide, together with geraniol, appears to be the main contributor for Gewürztraminer's typical rose aroma (Ong & Acree, 1999). Indeed, *cis*-rose oxide has a lower olfactory threshold (0.2 µg/l) than the *trans* isomer, with a more intense aroma of the tallest tea roses (Chigo-Hernandez et al., 2022).

During the aging process and depending on the storage conditions and wine oenological parameters (temperature and pH), the above-mentioned compounds participate in reactions, and the volatile compounds profile of the wines is enriched with cyclic and bicyclic terpenes (1,8-cineole, *trans*-terpin, α -terpineol, etc.). Some of these rearrangement or oxidation reactions are known to be acid-catalyzed and lead to an increase in cyclic forms and/or hydroxylated groups. Usually the open-chain monoterpene alcohols have a lower perception threshold than their cyclic equivalents, and this accounts for the reduction in the typical floral aroma during storage or aging.

Previously, we applied a fast GC–MS/MS method for the quantitation of dozens of wine volatile compounds in seven young Gewürztraminer wines, to observe their behavior during accelerated aging at 50 °C. Among others, it was pointed out that linalool, nerol, and geraniol decreased, while some volatile cyclic and bicyclic terpenes, such as α -terpineol and 1,8-cineole, increased (Carlin et al., 2022).

The knowledge of the chemical behavior of the VOCs (Volatile Organic Compounds) is of great importance for the enologists and wine scientists. Enologist can partially adjust the pH value of the juice and/or of wine during the winemaking and choose the temperature (T) for the wine storage, at least during the evolution in tanks and then the final ageing in bottle at the winery, before the wine is put on the market. However, in order to predict how the wine composition will develop during ageing under the influence of these factors, it is crucial to model the kinetics of these reactions in the real matrix. Such studies can provide us with important information about the reaction mechanisms and give us quantitative values about how the modulation of the storage temperature or wine pH can modify wine's VOCs stability and evolution. Such information can create important tools for the enologist in order to make decisions in concert to the wine style, the packaging or the application of certain enological practices (Piergiovanni et al., 2023; Sánchez-Acevedo et al., 2024). For what concerns the pH value, enologist can deliberately choose to produce wines with pH variable within the range 3.0–3.8, since the perceived sourness of this beverage is correlated with the titratable acidity (Plane et al., 1980), which is usually in the range 5–8 g/l of tartaric acid equivalents. This is a key observation, since the terpenoids in mature Gewürztraminer grapes are mainly present in the skins, and a maceration step before the alcoholic fermentation is often considered in order to increase the extraction of both free and bound monoterpenols, which is also resulting in Gewürztraminer wines with higher pH value.

Our study was planning considering that wine is often subjected to long maturation and storage, and that during its commercialization and transport the environmental conditions may vary from low temperature to 40, 50 °C or even higher.

Our kinetic investigation is aimed to provide insights into mechanistic aspects of the chemical interconversion among mono-terpenoids present in the wine here considered. Moreover, by collecting robust and reliable thermodynamic and kinetic parameters on these processes,

we aimed to give to the wine chemist useful information in several aspect related to wine storage. As reported in previous studies (Baxter et al., 1978; Cori et al., 1986; Poulter & King, 1982b, 1982a), the formation and/or disappearance of these metabolites during time promptly occur (at any given temperature and pH) mainly due to their involvement in both acid catalyzed (reversible) isomerization and (irreversible) cyclization steps.

2. Material and Methods

2.1. Experiment

The wine selected for this study was a premium-quality, young Gewürztraminer wine (Fondazione Edmund Mach Winery, Italy) from the 2020 harvest and sampled from the tank, before bottling in June 2021, and the storage experiment started the day after. The starting wine (10 L) had a pH of 3.83; the pH was lowered by adding sulfuric acid (Merck KGaA, Darmstadt, Germany) to pH 3.31 for the first batch and to pH 2.83 for the second batch. For each pH value, 30 bottles of 100 mL without headspace were filled, then closed with a screw cap, and placed in vacuum-sealed plastic bags with the addition of suitable powder (microbiology Anaerocult™ A produced by Sigma-Aldrich) to bind any oxygen remaining inside the package. The wine sampling, pH adjustment, homogenization, and bottle filling took place in an anoxic glove box (Jacomex, France). The bags containing the bottles were placed in stoves at five different temperatures: 25, 30, 35, 40, and 45 °C. The evolution during storage was monitored at five different time points (1, 2, 4, 8, and 15 days) plus 0 time for controls. To verify the effect of discontinuous heat on the wine, some bottles were also monitored by placing them in the respective stove and then removing them every other day to be left in the cold room. Two middle points of the experimental design were made in triplicate (pH 3.83, 35 °C, 4 days; and pH 3.31, 35 °C, 4 days). After completing their time in the stove, the bottles were transferred to a refrigerated cell at a temperature of 4 °C and positioned horizontally in a dark environment. The sample preparation and GC–MS/MS analyses were performed on the same day at the end of the experiments.

2.2. Sample preparation and extraction

Sample preparation and extraction of the free aroma compounds were performed according to the method described in Carlin et al. (2022). Solid-phase extraction was performed using Isolute® ENV+ (Biotage, Uppsala, Sweden) cartridges filled with 200 mg of stationary phase and pre-conditioned with 4 mL of dichloromethane, followed by 4 mL of methanol and 4 mL of model wine. A total of 50 mL of wine mixed with 100 mL of internal standard (n-heptanol 250 mg/L) was loaded onto the cartridge, which was then washed with 3 mL of water. The cartridges were dried for 10 min and eluted with 2 mL of dichloromethane directly into the injection vials.

2.3. GC–MS/MS analysis

The Agilent Intuvo 9000 system for fast GC coupled with an Agilent 7010B triple quadrupole mass spectrometer (Agilent Technologies, Santa Clara, CA, USA) equipped with an electronic ionization source operating at 70 eV were used for the analysis. Separation was achieved by injecting 1 µL in split mode (1:10) into a DB-Wax Ultra Inert column (30 m × 0.25-mm id × 0.25-µm film thickness, Agilent Technology, Santa Clara, CA, USA). The GC oven's initial temperature was 40 °C for 2 min, ramped up by 10 °C/min to reach 55 °C, then by 20 °C/min until 165 °C, by 40 °C/min to 240 °C for 1.5 min, and finally by 50 °C/min to 250 °C and kept at this temperature for an additional 4 min (16 total runtime). Helium was used as the carrier gas (with a flow of 1.2 mL/min). The mass spectra were acquired in multiple reaction monitoring modes. Nitrogen was used as the collision gas, with a flow of 1.5 mL/

min, in addition to helium at 4.0 mL/min as the quench gas. The transfer line and source temperature were set at 250 °C and 230 °C, respectively. The MRM parameters can be found as [Supplementary Material Table S1](#). The data acquisition and subsequent quantification analyses were performed using the MassHunter Workstation software (Agilent Technologies, Santa Clara, CA, USA) as previously described ([Carlin et al., 2022](#)).

2.4. Kinetic data analysis

Two main approaches are usually followed when dealing with kinetic investigations; the first one is a purely phenomenological/empirical approach whereby the time change of the concentration of any interesting metabolite is measured by a given analytical method, collecting a set of $C_i(t)$ at different times. Assuming first order (or pseudo first order) kinetic laws, by following the time change of the logarithmic ratio (S) between the actual concentration of the *i*-esime metabolite ($C_i(t) - C_i(0)$) and its initial concentration $C_i(0)$ (i.e., $S_i(t) = \ln [C_i(t) - C_i(0)/C_i(0)]$) at any given T and pH , it simply deals with the linear equation $S_i(t) = -(k_{obs}t)_i$ where k_{obs} (in s^{-1} if time course is measured in seconds) represents the empirical rate constant of the overall process wherein *i*-esime metabolite is involved. However, the values of these empirical k_{obs} are a complex function of the true rate constant k_i regulating the elementary step whereby that compound appears (or disappears if a reagent) and thus k_{obs} is devoid of any mechanistic significance.

We followed another approach, theoretically-based, which requires the definition of a complete system of ordinary differential equations (ODE) with well-established boundary conditions (initial concentration of reactants/products). Basically, this ODE system deals with a specific first order (or pseudo first order) kinetic law for any given elementary step since chemical species such as H_2O or H_3O^+ are present in large molar excess in buffered wine with respect the secondary metabolites investigated. The integrated kinetic laws (simultaneous solutions of these ODE) thus represent the time history of the chemical system under investigation.

To find the analytical solutions of these equations, however, it is all but an easy task. In order to evaluate the unknown rate constants (k_i $i = 0, 1, n$) it is necessary to resort to rigorous and accurate stochastic algorithms able to propagate reactions evolution and to allow accurate simulations of the experimental kinetic data. Kinetiscope (version 1.1.1136) was used as the kinetic simulation software. ([Gillespie, 2007](#)). After evaluating the different k_i at different temperatures (and at given pH), activation energy of any elementary step can be obtained by the Arrhenius plot ($\ln k_i$ versus $1/T$) although it is usually better to resort to Eyring equation: $k_i = k_B T/h \exp(-\Delta G_i^\ddagger/RT)$ where k_i is the rate constant of the *i*-esime elementary step considered, k_B is the Boltzmann constant (1.38×10^{-23} J/K), h is the Planck constant (6.63×10^{-34} J*s) and ΔG_i^\ddagger is the free energy of activation of the same process. Eyring equation is based on statistical mechanical foundations (whereas Arrhenius equation is purely empirical) and allow to factorize the two independent contributions at the change in Gibbs free energy ΔG^\ddagger as the activation enthalpy (ΔH^\ddagger) and the activation entropy (ΔS^\ddagger). Within this approach, by knowing the rate constant of the *i*-esime process at a given temperature $k_i(T)$, its ΔG^\ddagger value at the same temperature is directly provided by the Eyring equation whilst ΔH^\ddagger can be accurately evaluated from the slope in the linear Eyring plot ($\ln(k_i/T)$ versus $1/T$). A rough estimation of the activation entropy term ΔS^\ddagger could be obtained by the intercept of the same plot but, since the standard deviation of the intercept is usually quite large in kinetics measurements (where the investigated temperature range is usually narrow), it is largely better to obtain ΔS^\ddagger from previously evaluated values of ΔG^\ddagger and ΔH^\ddagger as $T\Delta S^\ddagger = \Delta H^\ddagger - \Delta G^\ddagger$. While E_a and ΔH^\ddagger are expected (and really found) to be quite similar in processes with high activation barriers ($E_a = \Delta H^\ddagger + RT$), different values are often obtained for ΔG^\ddagger and ΔH^\ddagger whenever the activation entropy term plays a relevant role, not a so uncommon findings in several organic reactions.

3. Results and Discussion

On the ground of previous literature data both from wine chemistry studies ([Fariña et al., 2005](#); [Rapp & Marais, 1993](#); [Slaghenaufi & Ugliano, 2018](#)) and from pioneering investigations on reactions mechanisms of these reactions ([Baxter et al., 1978](#); [Cori et al., 1986](#)) we propose here a reasonable mechanism for these isomerization/cyclization reactions of monoterpenoids in our wine ([Fig. 1](#)) where, basically, the key intermediate linalool is both engaged in reversible isomerization equilibria with geraniol and nerol and subjected to a series of competitive irreversible cyclization processes leading mainly to α -terpineol and linalool oxides.

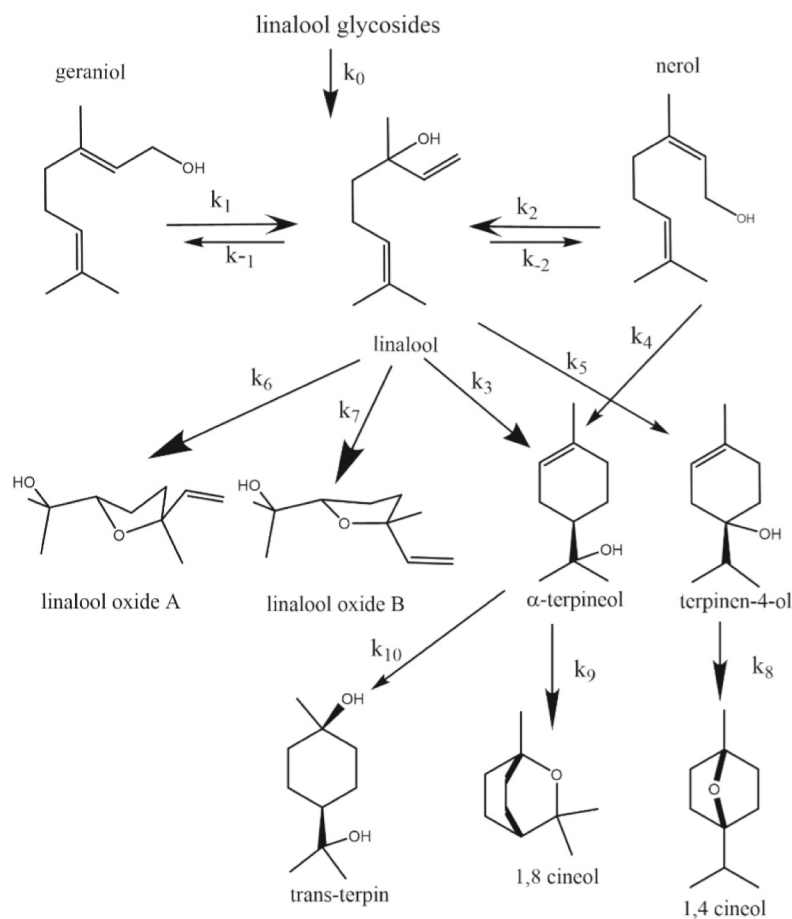
The aim of our work was to collect robust kinetic data for all the metabolites outlined in [Fig. 1](#) through GC-MS/MS measurements at 5 different temperatures 298 K (25 °C), 303 K (30 °C), 308 K (35 °C), 313 K (40 °C) and 318 K (45 °C) and at 3 different pH values (2.83, 3.31 and 3.83) in order to establish not only a comprehensive and reliable timescale of their fate in wine but also robust thermodynamic and kinetic data of these interconversions. The full data set and the technical variability of the protocol can be found in [Supplementary Tables S2–S3](#). This aim, as already outlined in the Introduction, must deal with the solutions of a system of ordinary differential equations that, in the case here examined, can be written as a system of 10 equations, as shown in [Fig. 1](#).

In order to find the solutions (k_i , $i = \pm 1, \pm 2, 3 \dots 10$) of the corresponding integrated equations $C_i(t)$ we resort to the software Kinetiscope ([Gillespie, 1976, 2007](#)) writing the above mentioned ODE and imposing the initial concentration of all our mono-terpenoids. However, we soon realized that it was almost impossible, at any given temperature, to find a set of k_i able simulate the experimental $C_i(t)$ curves. In fact, the required mass balance among monoterpenoids was not fulfilled since the total concentration of all the end-products at the latest timepoint (15 days or 1.296×10^6 s) was found in our experiments significantly higher than the total concentration of all the initial monoterpenoids. This finding strongly suggests that a simultaneous formation of free monoterpenoids, reasonably due to the hydrolysis of the corresponding glycosyl derivatives, is occurring on the same timescale of all the isomerization/cyclization processes. This outcome is not surprising since, from one hand, glycosyl terpenoids are present in high relative abundance in Gewürztraminer wines and, from the other hand, the acid catalysed hydrolysis of tertiary terpenoid is expected to occur with rate constants $k_{hydrolysis}$ similar to isomerization/cyclization processes. A journey through the early literature on the subject ([Timell, 1964](#)) pointed out that acid hydrolysis of alkylglycosides glycosyl-O-R occurs quite slowly, generally requiring strong experimental conditions ($T > 60^\circ C$, $pH < 2$) in order to be observed, no matter of the length of the alkyl chain considered. However, when dealing with tertiary alkyl group (for example *t*-butyl group) the hydrolysis of the corresponding glycosyl-O-CR₃ becomes much faster, 500 times for *t*-butyl –C(Me)₃ and till 30,000 times faster for –C(Et)₃ glycosides, possibly due to different mechanism followed in this case. The increase of the hydrolytic rate constant is so high that the acid-catalysed hydrolysis of these glycosides can be observed even at the experimental conditions of our kinetic runs ($T \geq 25^\circ C$, $pH \geq 2.83$). Since the only monoterpenoid-glycosides containing a tertiary carbon atom linked to O-glycoside moiety are the linalool and α -terpineol glycosides (glycosyl-O-C(Me)RR') we explicitly added this process ([equation A](#), regulated by the rate constant k_0 , in order to ensure a correct mass balance. With such an assumption the kinetic law 3. ([Fig. 1](#)) must change in the updated [equation B](#), as here reported

$$-d[\text{linaloolglycosides}]/dt = k_0[\text{linaloolglycosides}] \quad (\text{A})$$

$$d[\text{linalool}]/dt = k_0[\text{linaloolglycoside}] + k_1[\text{geraniol}] + k_2[\text{nerol}] - (k_3 + k_5 + k_6 + k_7)[\text{linalool}] \quad (\text{B})$$

Considering that linalool is a chemical precursor of α -terpineol and



1. $-d[\text{geraniol}]/dt = k_1[\text{geraniol}] + k_{-1}[\text{linalool}]$
2. $-d[\text{nerol}]/dt = (k_2 + k_4)[\text{nerol}] + k_{-2}[\text{linalool}]$
3. $d[\text{linalool}]/dt = k_1[\text{geraniol}] + k_2[\text{nerol}] - (k_3 + k_5 + k_6 + k_7)[\text{linalool}]$
4. $d[\text{linalool-oxide A}]/dt = k_6[\text{linalool}]$
5. $d[\text{linalool-oxide B}]/dt = k_7[\text{linalool}]$
6. $d[\text{terpinen-4-ol}]/dt = k_5[\text{linalool}]$
7. $d[\alpha\text{-terpineol}]/dt = k_3[\text{linalool}] + k_4[\text{nerol}] - (k_8 + k_9)[\alpha\text{-terpineol}]$
8. $d[\text{trans-terpin}]/dt = k_{10}[\alpha\text{-terpineol}]$
9. $d[1,8\text{-cineol}]/dt = k_9[\alpha\text{-terpineol}]$
10. $d[1,4\text{-cineol}]/dt = k_8[\text{terpinen-4-ol}]$

Fig. 1. The reactions of monoterpenoids occurring in wine and subject of the present study.

exists in equilibrium with geraniol and nerol species, we use only the linalool glycosides as an additional source of mono-terpenoid. If we assume, on the basis and in agreement with literature data (D'Onofrio et al., 2017; Katarína et al., 2014), that i) the initial concentration of this glycosides is about 200 $\mu\text{g/L}$, ii) the hydrolytic rate constant of linalool-glycosides (k_0) is $1.00 \times 10^{-7} \text{ s}^{-1}$ at $T=303 \text{ K}$ and $\text{pH} 2.83$, then all the mass balances in our kinetic run were promptly fulfilled. Things do not change significantly in our simulations if we consider a contribute of the hydrolysis of α -terpineol glycosides but under the mass balance constrain that the overall initial concentration of linalool-+ α -terpineol glycosides is 200 $\mu\text{g/L}$.

Just as example, to better illustrate how the relevant 13 kinetic

parameters (k_i , $i = 0, \pm 1, \pm 2, 3, \dots, 10$) have been evaluated, we illustrate in some detail the kinetic data collected at $\text{pH} 2.83$. The same approach was used to evaluate these kinetic parameters at different pH values (3.31 and 3.83).

Fig. 2A shows the experimental data concerning the time change of concentrations of all the monoterpenoids along 15 days ($\text{pH} 2.83$) whilst in Fig. 2B are shown the integrated curves $C_i(t)$ as obtained by Kineticscope software. In all the simulations the initial concentrations of monoterpenoids were taken by GC-MS/MS experimental data as the following: linalool glycoside 200 $\mu\text{g/L}$, geraniol 270 $\mu\text{g/L}$, nerol 88 $\mu\text{g/L}$, linalool 163 $\mu\text{g/L}$, α -terpineol 50 $\mu\text{g/L}$, linalool oxide A 13 $\mu\text{g/L}$, linalool oxide B, 8 $\mu\text{g/L}$, *trans*-terpin 4 $\mu\text{g/L}$, terpinen-4-ol 2 $\mu\text{g/L}$, 1,4-cineole

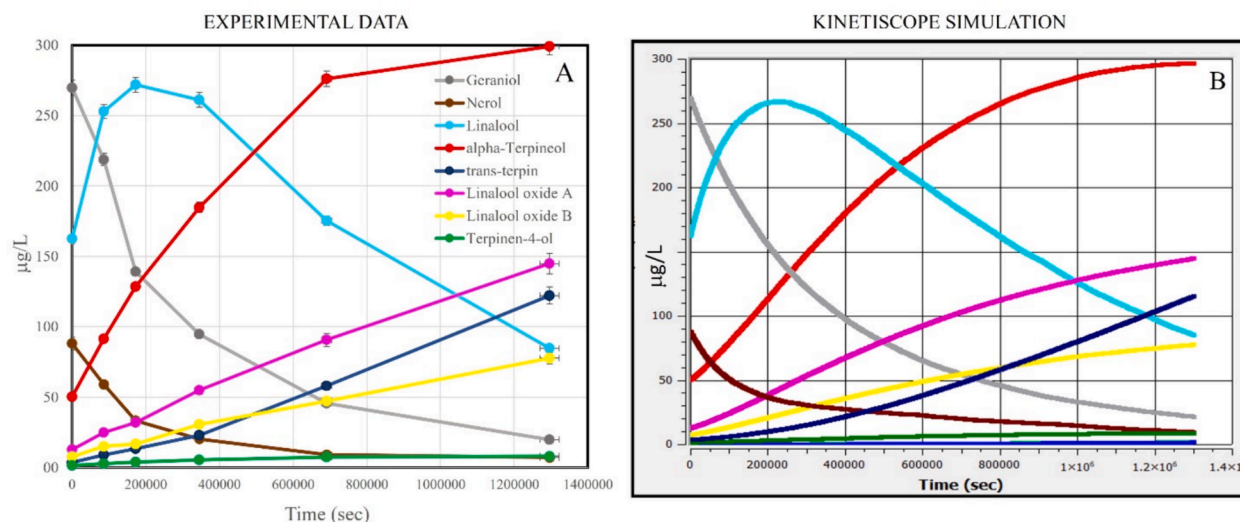


Fig. 2. (A) Kinetic data of major monoterpenoids as measured by GC-MS/MS at T=318 K and pH 2.83, (B): Kinetic data of the major monoterpenoids as evaluated by integrated differential equations with the stochastic simulator Kinetiscope software at T=318 K and pH 2.83.

0.08 µg/L and 1,8-cineole 0.003 µg/L. The final set of the rate constants k_i were obtained after few trials by modifying their values until an optimal agreement between the calculated and the experimental curves $C_i(t)$ was found.

At 318 K and pH 2.83 the best fitting k_i values for the equilibrium among linear monoterpenols are $k_0 = 1.4 \times 10^{-6} \text{ s}^{-1}$, $k_1 = 3.0 \times 10^{-6} \text{ s}^{-1}$, $k_{-1} = 3.8 \times 10^{-7} \text{ s}^{-1}$, $k_2 = 2.5 \times 10^{-6} \text{ s}^{-1}$ and $k_{-2} = 1.4 \times 10^{-7} \text{ s}^{-1}$ where the best k_i for cyclization processes are $k_3 = 1.3 \times 10^{-6} \text{ s}^{-1}$, $k_4 = 1.9 \times 10^{-6} \text{ s}^{-1}$, $k_5 = 4.5 \times 10^{-8} \text{ s}^{-1}$, $k_6 = 5.4 \times 10^{-7} \text{ s}^{-1}$, $k_7 = 2.9 \times 10^{-7} \text{ s}^{-1}$, $k_8 = 2.5 \times 10^{-7} \text{ s}^{-1}$, $k_9 = 5.7 \times 10^{-9} \text{ s}^{-1}$ and $k_{10} = 4.1 \times 10^{-7} \text{ s}^{-1}$. As a rough estimate of accuracy, we can safely establish that their relative errors are not higher than 3 %, thus for example $k_1 = (3.0 \pm 0.1) \times 10^{-6} \text{ s}^{-1}$. Since the overall rate of forward processes ($k_0 + k_1 + k_2$) leading to linalool is about 13 times higher than the rate of backward reactions leading to geraniol and nerol ($k_{-1} + k_{-2}$) and about 3 times higher than the conversion of linalool itself ($k_3 + k_5 + k_6 + k_7$) into cyclized end-products, linalool accumulates in the early part of the run but, after about 5–6 h its irreversible conversion in cyclized products (in particular in α -terpineol) overrides its formation. According to these evaluated k_i , after about 14 h (5×10^4 sec), $[\alpha\text{-terpineol}] = [\text{linalool}]$ and $[\text{geraniol}] = [\text{linalool oxide A}]$ whilst $[\text{nerol}]$ is almost negligible, an outcome in fair agreement with the experimental data (Fig. 2A). Thus, in a few days a complete rewiring of monoterpenoids occurs, geraniol, nerol and linalool become minor metabolites whilst α -terpineol, linalool oxides and *trans*-terpin become the most abundant metabolites as shown in the last timepoint of our kinetic run (15 days). Our simulation allows to establish that, at this low pH value, just after 1 month at T=318 K, the major metabolite becomes *trans*-terpin (260 µg/L) followed by α -terpineol (225 µg/L), linalool oxide A (170 µg/L), and linalool oxide B (94 µg/L) whilst linalool (13 µg/L), geraniol (3 µg/L) and nerol (0.5 µg/L) are almost totally disappeared, 1,4-cineole increases its presence (and their characteristic fragrances) till 6–7 µg/L as well as 1,8-cineole till 2–3 µg/L. However at T=298 K (pH 2.83) after 1 month the scenario is totally different: the major metabolites should be linalool (260 µg/L), α -terpineol (150 µg/L) and geraniol (110 µg/L), followed by linalool oxide A (40 µg/L), nerol (28 µg/L), linalool oxide B (20 µg/L) and *trans*-terpin (15 µg/L) with cineols still at trace level (0.1–0.3 µg/L).

The Eyring analysis of the data in Table 1 affords the relevant kinetic parameters reported in Table 2.

Several remarks are worth of note by analysing the kinetic parameters at the pH 2.83, reported in Table 2. In particular, the hydrolysis of linalool glycosides shows free energy of activation ($\Delta G^\ddagger = 114.2 \text{ kJ/mol}$) in the average values observed for almost other chemical processes

Table 1

Kinetic constant (s^{-1}) at pH=2.83 as evaluated by simulation of the integrated differential equations outlined in Fig. 1.

s^{-1}/K	298	303	308	313	318
k_0	8.00E-08	2.0E-07	2.80E-07	6.00E-07	1.40E-06
k_1	4.10E-07	7.00E-07	1.00E-06	2.00E-06	3.00E-06
k_{-1}	5.00E-08	8.00E-08	1.30E-07	2.50E-07	3.80E-07
k_2	4.60E-07	7.50E-07	1.10E-06	1.60E-06	2.50E-06
k_{-2}	2.50E-08	3.30E-08	5.40E-08	7.20E-08	1.40E-07
k_3	1.60E-07	2.80E-07	3.80E-07	9.00E-07	1.30E-06
k_4	1.20E-07	3.00E-07	3.80E-07	8.50E-07	1.90E-06
k_5	2.00E-09	7.50E-09	1.00E-08	2.60E-08	4.50E-08
k_6	4.30E-08	7.50E-08	1.05E-07	2.60E-07	5.40E-07
k_7	2.40E-08	3.80E-08	5.80E-08	1.30E-07	2.90E-07
k_8	3.50E-08	6.50E-08	1.20E-07	2.00E-07	2.60E-07
k_9	4.50E-10	9.00E-10	1.60E-09	3.00E-09	5.70E-09
k_{10}	4.30E-08	9.70E-08	1.40E-07	2.50E-07	4.10E-07

where $108.9 < \Delta G^\ddagger < 122.6 \text{ kJ/mol}$ but, on the contrary, it shows an enthalpy of activation ($\Delta H^\ddagger = 99 \text{ kJ/mol}$) significantly higher of other reactions where $62 < \Delta H^\ddagger < 83 \text{ kJ/mol}$. In kinetic terms, it implies that the rate constant k_0 increases much more than other k_i by increasing the temperature. A useful empirical parameter used to define this outcome is Q_{10} , the k_0 increase factor for a temperature change $\Delta T = 10 \text{ K}$ in the range 298–308 K. For this process it can be easily evaluated by Eyring equations to be $Q_{10} (298\text{K} \rightarrow 308\text{K}) = 4.1$ (and, similarly $Q_{20} (298\text{K} \rightarrow 318\text{K}) = 16.3$). Thus, although k_0 at 298 K ($k_0 = 8.0 \times 10^{-8} \text{ s}^{-1}$, i. e. $t/2 \approx 100$ days) is lower than k_1 , k_2 and k_3 , it become very similar to them at 318 K. In short, acid hydrolysis of glycosides is relevant at high temperature, but it is almost negligible around r.t. (298 K) and become negligible ($1.7 \times 10^{-8} \text{ s}^{-1}$, i. e. $t/2 \approx 470$ days) at 290 K. This finding confirms the practical importance of the storage of aromatic wines at low temperature, described in the Introduction section.

Concerning the isomerization equilibria among geraniol/linalool/nerol species, our approach allows to define not only the corresponding rate constants but also, under reasonable assumption, to establish the equilibrium constants of both geraniol/linalool's isomerization $K_{\text{eq}} = [\text{L}]/[\text{G}]$ (at 298 K $K_{\text{eq}} = k_1/k_{-1} \approx 8.2$, i.e. $\Delta G_{\text{R}}^0 = -5.2 \text{ kJ/mol}$) and of linalool/nerol's isomerization $K_{\text{eq}} = [\text{N}]/[\text{L}]$ (at 298 K $K_{\text{eq}} = k_{-2}/k_2 = 0.055$, i.e. $\Delta G_{\text{R}}^0 = +7.2 \text{ kJ/mol}$). Hence, the equilibrium between geraniol and nerol is regulated by the products of these equilibrium constants, i.e. $K_{\text{eq}} = [\text{N}]/[\text{G}]$ (298 K) = $k_1/k_{-1} * k_{-2}/k_2 = 0.45$ (i.e. $\Delta G_{\text{R}}^0 = +2.0 \text{ kJ/mol}$). This K_{eq} value is in nice agreement with the only (at the

Table 2

Kinetic parameters evaluated at pH 2.83, pH 3.31 and 3.83. ΔH^\ddagger values evaluated by Eyring plot, ΔG^\ddagger values calculated by Eyring equation at 298 K and $T\Delta S^\ddagger$ values evaluates as $T\Delta S^\ddagger = \Delta G^\ddagger - \Delta H^\ddagger$ at $T=298$ K (the correlation coefficients r^2 are in Table S4).

Elementary Process	ΔG^\ddagger (kJ/mol)			ΔH^\ddagger (kJ/mol)			$T\Delta S^\ddagger$ (kJ/mol)			ΔS^\ddagger J/molK		
	pH 2.83	pH 3.31	pH 3.83	pH 2.83	pH 3.31	pH 3.83	pH 2.83	pH 3.31	pH 3.83	pH 2.83	pH 3.31	pH 3.83
k_0	114.2	116.0	–	99.0	72.4	–	–15.2	–43.6	–	–51	–146.1	–
k_1	110.2	113.5	118.9	76.7	88.1	109.9	–33.5	–25.4	–3.56	–112	–85.2	–11.4
k_{-1}	115.4	118.8	124.0	79.3	83.5	120.9	–36.1	–35.3	1.99	–121	–118.4	6.3
k_2	109.9	113.5	118.5	62.7	66.0	106.8	–47.1	–47.5	–17.22	–158	–159.5	–55.0
k_{-2}	117.1	120.9	126.5	63.9	60.2	83.9	–53.2	–60.7	–34.64	–179	–203.9	–110.7
k_3	112.5	115.0	121.1	80.9	74.8	59.1	–31.6	–40.2	–67.40	–106	–135.0	–215.3
k_4	113.2	116.0	118.7	104.3	107.2	86.5	–8.9	–8.8	–34.61	–30	–29.4	–110.6
k_5	123.4	127.5	121.5	117.8	120.5	90.7	–70.4	–7.0	–27.97	–236	–236.4	–89.4
k_6	115.8	117.7	123.0	96.5	92.4	99.1	–19.2	–25.3	–22.36	–65	–84.9	–71.5
k_7	117.2	119.4	130.7	95.1	89.5	98.6	–22.2	–29.9	–24.40	–74	–100.5	–78.0
k_8	116.3	116.0	124.0	78.5	106.5	110.8	–37.8	–9.5	–70.44	–127	–31.8	–225.1
k_9	127.2	133.2	135.8	96.4	105.1	85.8	–30.8	–28.1	–38.25	–103	–94.4	–122.2
k_{10}	115.8	117.2	124.2	83.5	85.0	96.4	–32.3	–32.2	–39.38	–108	–108.1	–125.8

best of our knowledge) experimental measure reported in literature (Semikolenov et al., 2003) where it was estimated, in Vanadium catalysed thermal decomposition of linalool at 413 K, to be 0.62. Recently in a paper by Yu Yang (Yang et al., 2023) thermodynamic data (ΔG_f°) of these monoterpenoids were evaluated by *ab initio* calculations at high level of theory (DFT, B3LYP, 6.31 + G(d), using a polarizable continuum model to account for solvent effects). ΔG_f° (nerol) was calculated to be 0.75 kJ/mol higher than ΔG_f° (geraniol); since $\Delta G_R^\circ = \Delta G_f^\circ$ (nerol) – ΔG_f° (geraniol) = 0.75 kJ/mol, it is obtained that calculated $K_{eq} = 0.73$, still in good agreement with our experimental data. Worth of note in both equilibria we found that $\Delta G_R^\circ = \Delta \Delta G^\ddagger$; in fact, ΔG_R° (G→L) = –5.1 kJ/mol whereas $\Delta \Delta G^\ddagger = \Delta G_1^\ddagger - \Delta G_{-1}^\ddagger = (110.2 - 115.4)$ kJ/mol = –5.2 kJ/mol telling us that the energy of the transition states (TS₁ and TS₋₁ in Fig. 3A) leading to the same carbocation intermediates is practically the same and that the linalool converts to geraniol in the backward direction slower than geraniol into linalool in the forward process just because linalool is thermodynamically more stable than geraniol.

Similarly, ΔG_R° (L→N) = +7.1 kJ/mol whereas $\Delta \Delta G^\ddagger = \Delta G_2^\ddagger - \Delta G_{-2}^\ddagger = (117.1 - 109.9)$ kJ/mol = +7.2 kJ/mol still indicating that transition states (TS₂ and TS₋₂ in Fig. 3B) leading to the same carbocation intermediate have the same energy or, in other words, that the linalool converts to nerol slower in the forward direction than nerol in backward process just because linalool is thermodynamically more stable than nerol.

Things are different, however, when considering the temperature dependence of the rate constants. Our analysis suggests that, although the free energies of activation ΔG^\ddagger of the forward conversion G→L and N→L are practically the same (110.2 kJ/mol and 109.9 kJ/mol, respectively), the corresponding enthalpies of activation ΔH^\ddagger are quite different (76.7 versus 62.7 kJ/mol). Thus, the rate constant k_1 (G→L step) increases 17 times by increasing the temperature from 298 to 318 K whereas the corresponding fold increase of k_2 (N→L step) is only 5.0. From a mechanistic point of view, this outcome relies on the different contribution of the activation entropy term $T\Delta S^\ddagger$ which is negative in both cases, but it is significantly higher for N→L (–47 kJ/mol) with respect to G→L process (–23 kJ/mol.) The same considerations hold for the backward processes thus leading to the general conclusion that the $T\Delta S^\ddagger$ term play a more significant role in the N/L conversion than in G/L conversion, somehow compensating the opposite trend of the ΔH^\ddagger term.

Finally, regarding the cyclization processes leading to α -terpineol and linalool oxides, the latter can be derived only by C–O–C cyclization on the linalool substrate whilst the former could be obtained by C–C ring closure both by linalool and nerol (Fig. 4). Focusing the attention on cyclization to α -terpineol, the driving force of this process is the total irreversibility due to the much higher thermodynamic stability of the cyclic product with respect to the linear terpenoids. This is mainly due to the fact that a weaker π bond at C(7)–C(8) in the reactants is converted in a stronger σ bond at C(1)–C(7) in the cyclized product. According to

recent *ab initio* calculations (Yang et al., 2023) the free energy of α -terpineol has been calculated to be about 72 and 78 kJ/mol more stable than linalool and nerol, respectively. Thus, the backward reactions in Fig. 4 are **totally forbidden** at ordinary temperatures. At 298 K, within the accuracies of our experimental measures and their Kinetoscope-based simulations, the rate constants regulating the cyclizations L→ α -T (k_3) and N→ α -T (k_4) have similar values ($k_3 = 1.6 \pm 0.1 \times 10^{-7} \text{ s}^{-1}$ versus $k_4 = 1.2 \pm 0.1 \times 10^{-7} \text{ s}^{-1}$), thus the corresponding processes have almost the same ΔG^\ddagger values (113.0 ± 0.2 kJ/mol). However, they show significantly different enthalpy of activation ($\Delta \Delta H^\ddagger = +23$ kJ/mol) allowing to explain that, at 318 K, k_4 overrides k_3 (45 %-fold increase); the opposite trend in the corresponding activation entropic term ($T\Delta \Delta S^\ddagger \approx 23$ kJ/mol) ensures the invariance of the free energy of activation ($\Delta \Delta G^\ddagger \approx 0$). Since linalool is about 7.2 kJ/mol more stable than nerol, the transition state TS₃ (Fig. 3A) must lie about 7.2 kJ/mol lower than transition state TS₄ (Fig. 3B) in order to explain our observations. What is more important, while at **low temperature (T ≤ 298 K) monoterpenoids are mainly engaged in fast isomerizations processes, at higher T irreversible cyclization becomes dominant.**

The O-cyclization of linalool to linalool oxides occurs on a slightly lower timescale (k_6 and k_7 are about 3 times slower than k_3 within 298–318 K range) than the C-cyclization of linalool/nerol to α -terpineol. In particular, the formation of the more stable linalool oxide A (*trans*-isomer) occurs a little bit faster (2 times) than the formation of its *cis* isomer and its concentration increases by increasing the temperature more than *cis*-isomer ($\Delta \Delta H^\ddagger \approx 7$ kJ/mol). Anyhow, the formation of these oxides is not an elementary process since it requires preliminary oxidation (epoxidation at the C(7) = C(8) double bond, not shown in our Figure) before cyclization, thus k_6 and k_7 (and their corresponding kinetic parameters) are not true rate constants of the cyclization processes but only observed rate constants embedding both the processes. These oxides are present in low concentration in Gewürztraminer (15–25 $\mu\text{g/L}$) but could become major metabolites (80–150 $\mu\text{g/L}$) for few days standing at 318 K and low pH values.

Even terpinen-4-ol seems to play a minor role in our investigation. Its rate constants ($k_5 = 3.6 \times 10^{-8} \text{ s}^{-1}$ at $T=318$) is so low even at high temperature that its final concentration is found lower than 10 $\mu\text{g/L}$ after 15 days.

More interesting is the kinetics of cineols, which are present in very low concentration in Gewürztraminer at 3–80 ng/L but become more significant ($\approx 2 \mu\text{g/L}$) on long standing at 318 K. According to our analysis, formation of 1,8-cineole is significantly slower at 298 K than that of 1,4-cineole (about 90 times) but increases at higher temperatures more than the latter. The analysis of their kinetic parameters indicates that $\Delta \Delta H^\ddagger$ (= ΔH^\ddagger (1,8-cineole)– ΔH^\ddagger (1,4-cineole)) is much higher (≈ 29 kJ/mol) than the corresponding $\Delta \Delta G^\ddagger$ (≈ 11 kJ/mol). Thus whereas formation of 1,8-cineole seems driven much more by enthalpic than entropic term ($\Delta H^\ddagger \approx 96$ kJ/mol and $T\Delta S^\ddagger \approx 30$ kJ/mol), in the

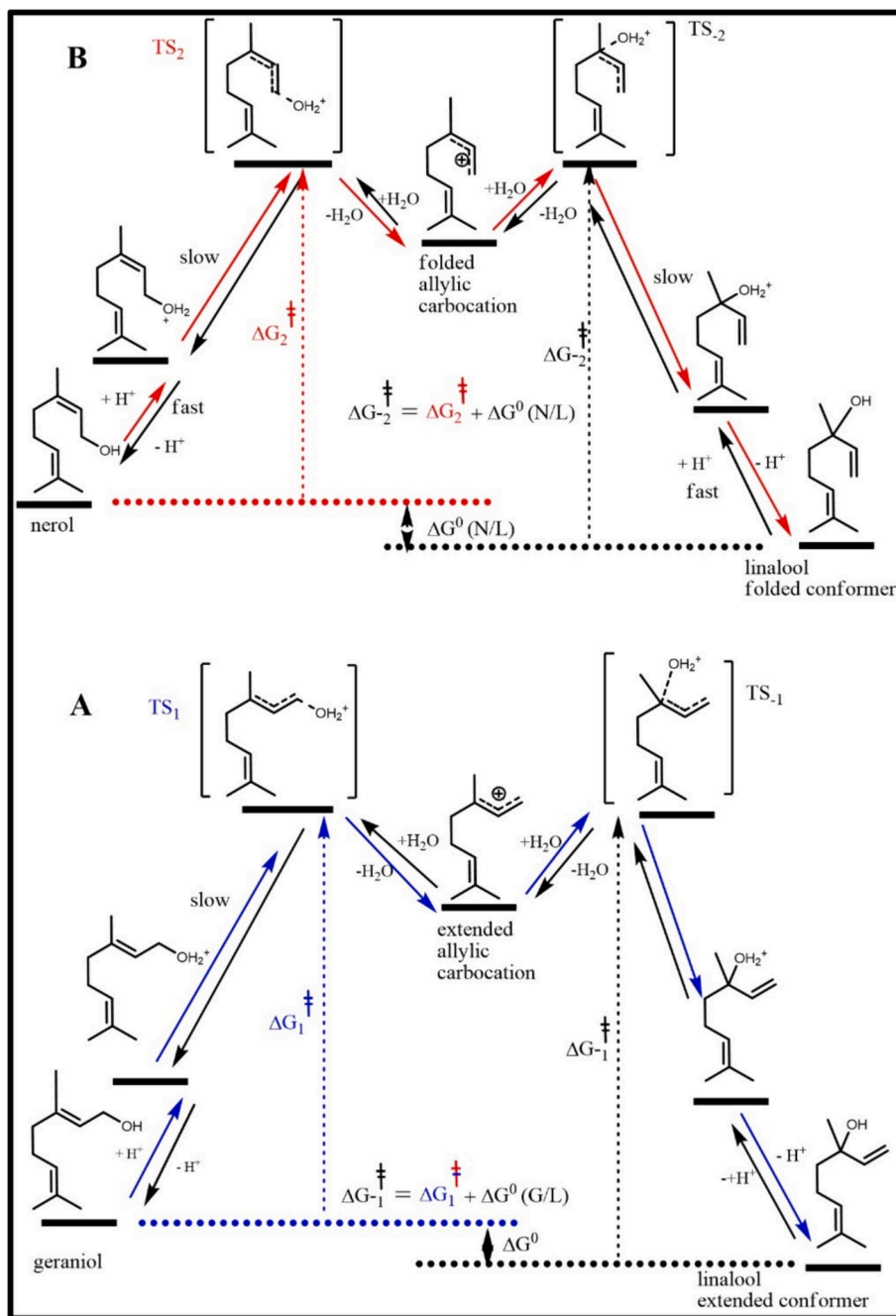


Fig. 3. Energy profile of the geraniol/linalool (A) and nerol/linalool (B) isomerization.

formation of the 1,4 isomer both terms seem to play similar weight ($\Delta H^\ddagger \approx 68$ kJ/mol and $T\Delta S^\ddagger \approx -47$ kJ/mol).

Also, for *trans*-terpin reliable and robust kinetic data have been obtained in our investigation. Its formation is simply due to acid-catalyzed water addition to the endocyclic double of α -terpineol and it increases from about 4 μ g/L till to 120 μ g/L after 15 days at 318 K. It represents, with cineols and linalool oxides, another **end-product** whereby chemistry could not work anymore.

pH dependence of k_i .

By applying the same approach, we were able to find the corresponding k_i values for kinetic runs carried out at pH 3.31 and pH 3.83 (Table 3 and Table S5). As expected, at any given temperature, for all the steps considered in Fig. 1 we observed that:

$$k_i(\text{pH } 2.83) > k_i(\text{pH } 3.31) > k_i(\text{pH } 3.83)$$

but not in all processes we observed the same trend. If the cyclization/isomerization processes here considered were subjected to specific acid catalysis it would be expected that $k_i(\text{pH } 2.83) \approx 3.1^* k_i(\text{pH } 3.31)$ and, similarly $k_i(\text{pH } 2.83) \approx 10^* k_i(\text{pH } 3.83)$ reflecting the corresponding higher concentration of H_3O^+ at pH 2.83 with respect pH 3.31 and pH 3.83, respectively.

Most of the processes here discussed seem actually to **strictly follow specific acid catalysis** since their rate constants, according to our simulations at pH 3.31, are about 3.0 ± 0.2 times slower than at pH 2.83. This k_i fold change correspond at $T=298$ K to a:

$$\Delta\Delta G^\ddagger (= \Delta G^\ddagger(\text{pH } = 3.31) - \Delta G^\ddagger(\text{pH } = 2.83)) = 2.84 \text{ kJ/mol}$$

as confirmed in Table 3.

The Eyring calculations for the pH 3.31 affords the relevant kinetic

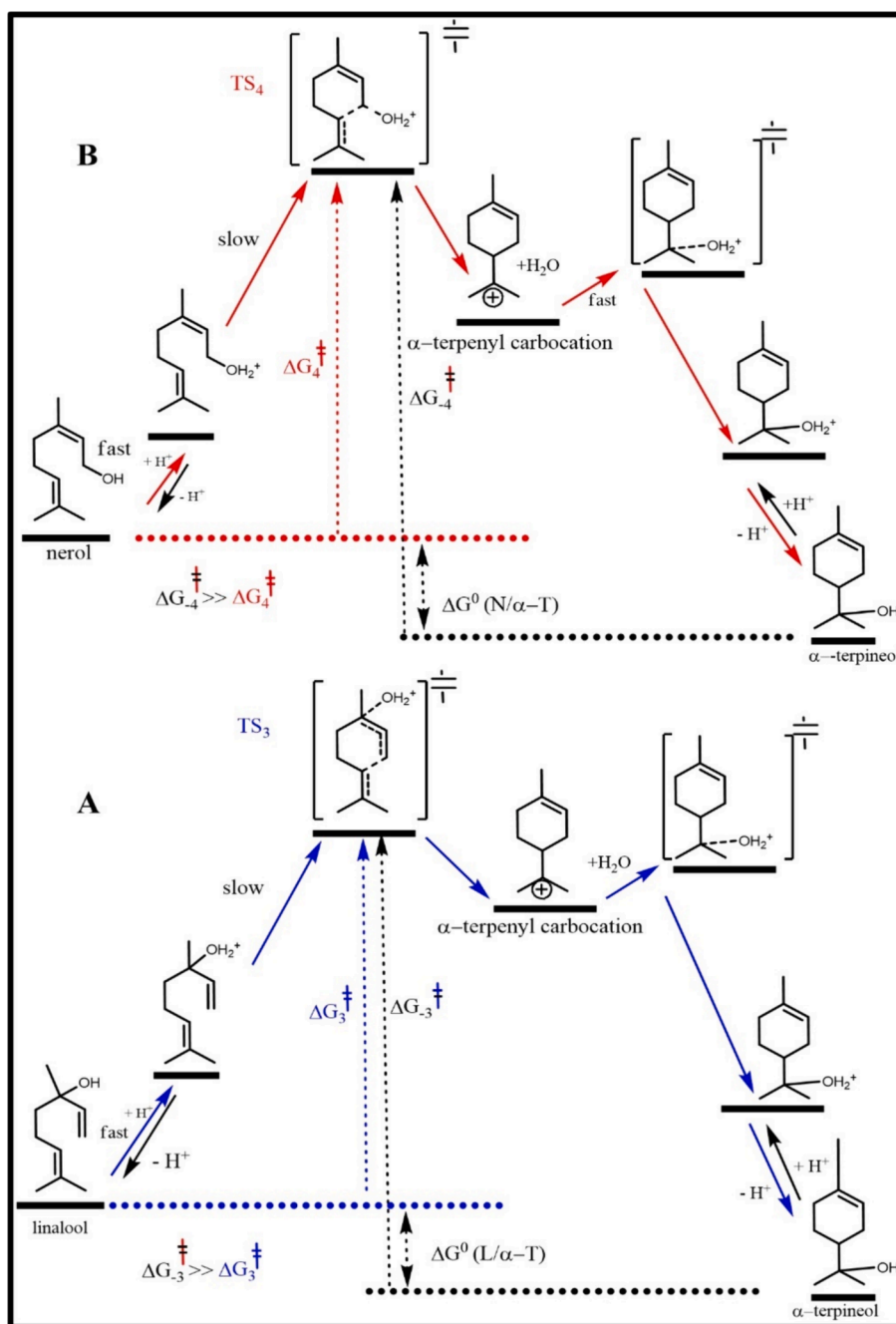


Fig. 4. Energy profile of the linalool/ α -terpineol (A) and nerol/ α -terpineol (B) cyclization.

parameters of all the steps outlined in Fig. 1 and are also reported in Table 2.

Fig. 5 collect all the experimental data and simulations of our kinetics runs within 298–318 K at pH 2.83, and in Figure S1 also those obtained at pH 3.31. Deviations from the calculated ratio 3.1 can be easily attributed to presence of random errors in experimental measures (including pH) and in theoretical simulations. More importantly, the $\Delta\Delta H^\ddagger$ ($=\Delta H^\ddagger(\text{pH}=3.31) - \Delta H^\ddagger(\text{pH}=2.83)$) values are widely distributed in different chemical processes ranging from significantly negative values (-26 kJ/mol for glycoside hydrolysis) to significantly positive values ($+28$ kJ/mol for 1,4-cineole production). As a consequence, the rates of some processes are much more temperature-dependent than others. A striking example are the two competitive formations of α -terpineol from linalool regulated by k_3 ($\Delta\Delta H^\ddagger \approx -6$ kJ/mol) and from nerol regulated by k_4 ($\Delta\Delta H^\ddagger \approx +6$ kJ/mol); thus, the production of

α -terpineol from nerol increases with temperature at pH 3.31 much more than at pH 2.83 while the opposite is true for its production from linalool. The main message for oenologists is that a Gewürztraminer wine with pH=3.3 (a usual pH value for a white wine) after 3 months storage at 318 K geraniol, nerol and even linalool (and its glycosides) are totally transformed in *trans*-terpin, α -terpineol, linalool oxide A and linalool oxide B with %molar fractions 55, 13.5, 20 and 10, respectively. Minor amount of 1,4-cineole ($\approx 1\%$, ≈ 11 $\mu\text{g/L}$) and 1,8-cineole ($\approx 0.6\%$, ≈ 6 $\mu\text{g/L}$) are also observed at this pH value.

The analysis of the experimental data collected at pH 3.83 was more difficult since, in particular at the lowest temperatures here investigated (298 and 303 K), these conversions were so low that high relative errors do not allow to evaluate reliable kinetic parameters. We present here only the kinetic data obtained from the kinetics run at $T=308, 313$ and 318 K (Fig. S2 and Table S5). As a comparison with pH=3.31, a

Table 3

Kinetic constant (s^{-1}) at pH=3.31 as evaluated by simulation of the integrated differential equations outlined in Fig.1.

s^{-1}/K	298	303	308	313	318
k_0	1.00E-07	1.90E-07	3.00E-07	4.50E-07	7.00E-07
k_1	1.30E-07	2.00E-07	3.40E-07	6.40E-07	1.30E-06
k_{-1}	1.60E-08	2.50E-08	5.00E-08	8.90E-08	1.30E-07
k_2	1.40E-07	2.10E-07	3.00E-07	5.00E-07	8.00E-07
k_{-2}	9.00E-09	1.30E-08	1.80E-08	2.80E-08	4.50E-08
k_3	6.50E-08	9.50E-08	1.50E-07	2.70E-07	4.50E-07
k_4	3.90E-08	1.00E-07	1.40E-07	3.50E-07	6.80E-07
k_5	6.00E-10	2.10E-09	3.00E-09	8.00E-09	1.40E-08
k_6	1.40E-08	2.50E-08	3.80E-08	8.00E-08	1.60E-07
k_7	8.00E-09	1.30E-08	2.20E-08	4.00E-08	8.50E-08
k_8	1.00E-08	2.00E-08	4.00E-08	9.00E-08	1.50E-07
k_9	1.20E-10	2.70E-10	5.00E-10	9.00E-10	2.00E-09
k_{10}	1.40E-08	3.10E-08	4.50E-08	8.00E-08	1.40E-07

Gewürztraminer wine with pH=3.83 (an upper limit value for this wine) after 3 months storage at 318 K geraniol, nerol and linalool are still present (4, 1 and 12 %, respectively) although in low amount whereas α -terpineol, *trans*-terpin, linalool oxide A, linalool oxide B and 1,4-cineole show % molar fractions 37, 13, 21 10 and 1, respectively.

3.1. Practical implications

The above-described results can provide several important messages to the winemakers, and especially important for those producing Gewürztraminer wines, due to its richness of glycosides. Undoubtedly, aim of a Gewürztraminer producer is to preserve, for the longest term possible, the key aroma compounds of the cultivar, geraniol and *cis*-rose oxide. These two monoterpenoids, together with other compounds that belong to the same class, during wine aging take part in several reactions of hydrolysis, isomerisation, and cyclization, driven by the reactivity of the initial terpenoid profile, the temperature of the storage and the pH of the wine. Given the Gewürztraminer's richness in glycosidic monoterpenoids, the acid hydrolysis to produce the volatile aglycons, and therefore to enhance wine aroma, is the first key reaction. Our kinetic analysis has provided an experimental confirmation of the role of glycosides as important precursors of aroma. Highlighting the fact that the node/bridge to pass from the bound to free form are the linalool's glycosides, due to linalool's -OH tertiary structure, with the low pH and high temperature to favour this pass. However, the formed linalool is not the final product and so the reaction, under wine conditions, cannot be considered reversible.

The first reactions taking place, after the hydrolysis, are the isomerization reactions between the free linear monoterpenoids: linalool, nerol and geraniol. As proven above, at low storage temperature the linear monoterpenoids are mainly engaged in fast isomerization processes, with linalool being favoured. However, as the temperature increases one more reaction type starts to occur, cyclization. These cyclization reactions, deliver volatile cyclic and bicyclic compounds with completely different aroma character, higher olfactory threshold, and higher stability. Since the cyclic and bicyclic monoterpenoids (α -terpineol, linalool oxide A, 1,8-cineole, 1,4-cineole and *trans*-terpin) are thermodynamically more stable, they are becoming the most abundant aroma compounds of the process, with the three linear monoterpenoids being almost consumed, after one month at pH 2.83 and 45 °C. To underline the importance of wine storage temperature, at 25 °C, which is still above the optimal storage temperature of 14–16 °C (or lower), after one month, linalool is the major aroma compound, geraniol is preserved, and cineols are at trace level. Of course, the pH 2.83 is uncommon to white commercial wines, but the situation at the typical white wine pH of 3.3 wasn't that much more prominent. The reaction rates are approximately three times slower, as predicted for an acid catalysed process. However, with a further increase at pH 3.83 and temperature below 303 K (30 °C) the monoterpenoids are not subjected

to significant isomerization and/or cyclization processes. In Table 4 are reported the half-time predictions for linalool, geraniol and nerol at different temperatures and at 3 pHs. The predicted half-times for the linear monoterpenoids at cellar temperature is drastically improved at the highest pH value, and suitable for the production of long-aged white wines. This finding clarifies why some Gewürztraminer winemakers empirically choose to produce premium wines with a pH 3.8, which enhance the potential to preserve their aroma even after prolonged storage.

It is important to underline that the most experienced winemakers, through empirical experience, have already understood that in producing Gewürztraminer, acidification procedures lowering the pH to typical levels for other white wines should be avoided. Opting for less acidic pH is crucial for the longevity of aromatic wines. We are now able to confirm how this empirical choice is not only scientifically sound but also completely appropriate and optimal. Thanks to the detailed explanation produced in this study, which examines the kinetics and thermodynamics of all the involved reactions, we now have a definitive explanation.

Furthermore, using the differential equations with the stochastic Kineticscope software it was possible the simulation of what could happen after 6 months of storage at different conditions (Fig. 6). To maintain a high geraniol content and consequently the rose note typical of this variety, it is essential to keep the pH above 3.5 and the storage temperatures below 298 K (25 °C).

Even if for rose oxides it was not possible to find a complete system of ordinary differential equations (ODE) with well-established boundary conditions (initial concentration of reactants/products), from our data it would seem that there were different behaviours between the two isomers. The behaviour of rose oxide over time had already been observed in a previous study, wherein the different wines exhibited a faster decrease in the *trans* isomer and a slower one in the *cis* (Carlin et al., 2022). This experiment also revealed that *cis* rose oxide, which is also the most abundant and important at a sensory level, seems to be quite stable over time (Fig. S3), while the *trans* isomer shows a rapid decrease, especially at the lowest pH and at the highest temperatures. This diversity of behavior may be due to the molecule's shape and, in particular, to the steric hindrance present in the *cis* form. In their article, (Miyazawa et al., 1995) observed that the biotransformation of rose oxide by *Aspergillus niger* has a much lower yield for the *cis* isomer.

4. Conclusions

In conclusion, this study allowed us to produce a complete data set describing the evolution of the terpenoid profile as a function of pH and temperature. It was therefore possible to produce a simultaneous calculation of all the main interconversion processes, whether reversible or not. The results allowed us to produce a detailed, robust experimental confirmation of the importance of pH and temperature factors, and indicate that the combination of the presence of high quantities of terpene glycosides, high pH and low temperature of storage are the ideal factors for preserving the aroma of premium quality Gewürztraminer wines over time.

CRedit authorship contribution statement

Panagiotis Arapitsas: Writing – original draft, Visualization, Validation, Supervision, Resources, Project administration, Methodology, Investigation, Formal analysis, Data curation, Conceptualization. **Silvia Carlin:** Writing – original draft, Visualization, Validation, Supervision, Resources, Project administration, Methodology, Investigation, Formal analysis, Data curation, Conceptualization. **Fulvio Mattivi:** Writing – review & editing, Funding acquisition, Conceptualization. **Attilio Rapaccioli:** Writing – review & editing, Formal analysis, Data curation. **Urška Vrhovsek:** Writing – review & editing, Funding acquisition. **Graziano Guella:** Writing – original draft, Visualization, Validation,

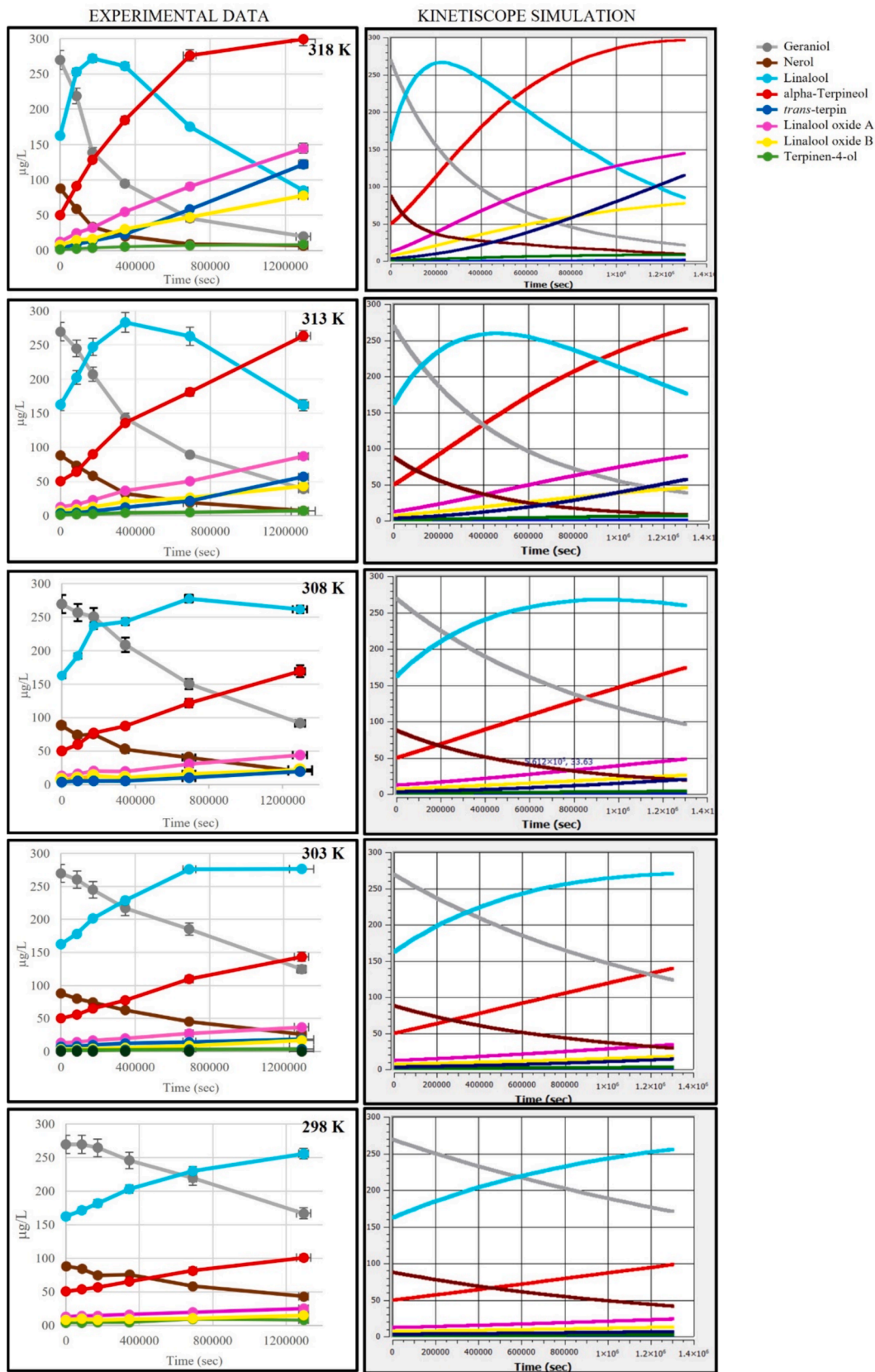


Fig. 5. Kinetic data (µg/L versus seconds) of major monoterpenoids as measured by GC-MS/MS technique at pH 2.83, according to the Kinetiscope simulations. (concentration in µg/L on the y-axis and time in second on the x-axis).

Table 4

Measured half-times (day) for the main linear terpenoids in Gewürztraminer wines at different temperatures and pH, and estimated half-times at cellar temperature, by assuming the same activation barrier.

pH	Terpenoid	Measured t/2 (day) of selected terpenoids at different temperatures and pH					Estimated t/2	
		298 K (25 °C)	303 K (30 °C)	308 K (35 °C)	313 K (40 °C)	318 K (45 °C)	293 K (20 °C)	288 K (15 °C)
2.83	geraniol	23	13	10	5	3	39	53
	nerol	17	10	7	4	2	29	43
	linalool	179	87	61	25	14	370	443
3.31	geraniol	72	46	35	15	8	111	149
	nerol	60	34	24	14	6	108	147
	linalool	414	197	177	76	46	870	970
3.83	geraniol	579	n.a	122	101	25	1620	2755
	nerol	113	n.a	39	27	13	227	327
	linalool	596	n.a	324	190	103	834	1097

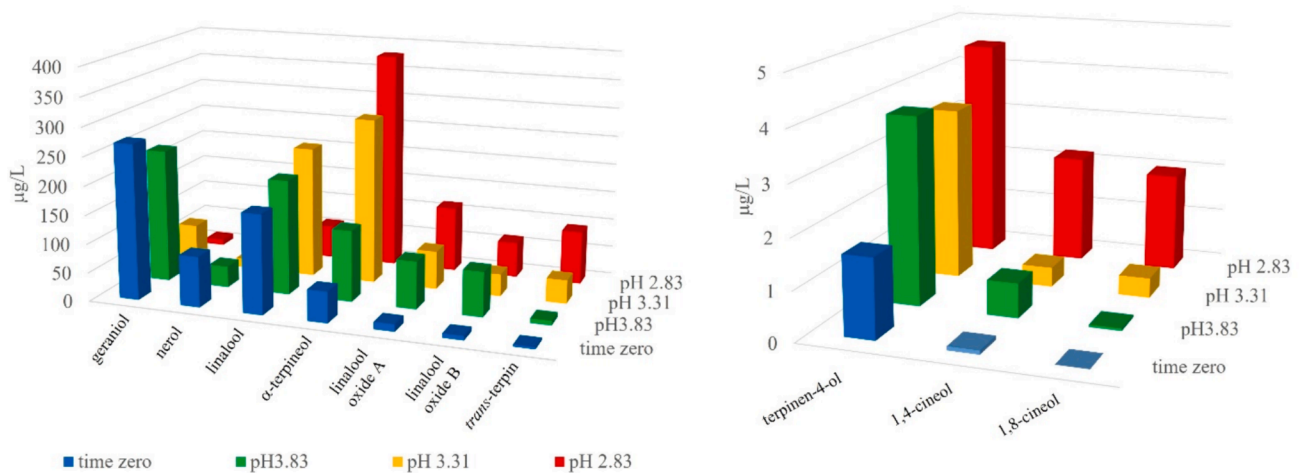


Fig. 6. Levels of major terpenoids after 6-month at different pH conditions and 298 K (25 °C), obtained using a simulation based on Kinetoscope model (concentration in µg/L on the y-axis, name of compounds on the x-axis, and pH values on the z-axis).

Supervision, Resources, Project administration, Methodology, Investigation, Formal analysis, Data curation, Conceptualization.

Declaration of competing interest

The authors declare that they have no known competing financial interests or personal relationships that could have appeared to influence the work reported in this paper.

Data availability

Data will be made available on request.

Acknowledgement

A special thank is due to the oenologists Willi Stürz, Enrico Pateroster and Gianni Gasperi for insightful discussion. The research was funded by the ERDF 2014–2020 Program of the Autonomous Province of Trento (Italy) with EU co-financing (Fruitomics).

Appendix A. Supplementary data

Supplementary data to this article can be found online at <https://doi.org/10.1016/j.foodres.2024.115017>.

References

Baxter, R. L., Laurie, W. A., & Mchale, D. (1978). Transformations of monoterpenoids in aqueous acids: The reactions of linalool, geraniol, nerol and their acetates in aqueous

- citric acid. *Tetrahedron*, 34(14), 2195–2199. [https://doi.org/10.1016/0040-4020\(78\)89026-7](https://doi.org/10.1016/0040-4020(78)89026-7)
- Carlin, S., Lotti, C., Correggi, L., Mattivi, F., Arapitsas, P., & Vrhovsek, U. (2022). Measurement of the Effect of Accelerated Aging on the Aromatic Compounds of Gewürztraminer and Teroldego Wines Using a SPE-GC-MS/MS Protocol. *Metabolites*, 12(2), 2. <https://doi.org/10.3390/metabo12020180>
- Chigo-Hernandez, M. M., DuBois, A., & Tomasino, E. (2022). Aroma Perception of Rose Oxide, Linalool and α -Terpineol Combinations in Gewürztraminer Wine. *Fermentation*, 8(1), 1. <https://doi.org/10.3390/fermentation8010030>
- Cori, O., Chayet, L., Perez, L. M., Bunton, C. A., & Hachey, D. (1986). Rearrangement of linalool, geraniol, nerol and their derivatives. *The Journal of Organic Chemistry*, 51(8), 1310–1316. <https://doi.org/10.1021/jo00358a028>
- D'Onofrio, C., Matarese, F., & Cuzzola, A. (2017). Study of the terpene profile at harvest and during berry development of Vitis vinifera L. aromatic varieties Aleatico, Brachetto, Malvasia di Candia aromatica and Moscato bianco. *Journal of Food and Agriculture*, 97(9), 2898–2907. <https://doi.org/10.1002/jsfa.8126>
- Fariña, L., Boido, E., Carrau, F., Versini, G., & Dellacassa, E. (2005). Terpene compounds as possible precursors of 1,8-cineole in red grapes and wines. *Journal of Agricultural and Food Chemistry*, 53(5), 1633–1636. <https://doi.org/10.1021/jf040332d>
- Ferretti, C. G., & Febbroni, S. (2022). Terroir Traceability in Grapes, Musts and Gewürztraminer Wines from the South Tyrol Wine Region. *Horticulturae*, 8(7), 7. <https://doi.org/10.3390/horticulturae8070586>
- Gillespie, D. T. (1976). A general method for numerically simulating the stochastic time evolution of coupled chemical reactions. *Journal of Computational Physics*, 22(4), 403–434. [https://doi.org/10.1016/0021-9991\(76\)90041-3](https://doi.org/10.1016/0021-9991(76)90041-3)
- Gillespie, D. T. (2007). Stochastic simulation of chemical kinetics. *Annual Review of Physical Chemistry*, 58, 35–55. <https://doi.org/10.1146/annurev.physchem.58.032806.104637>
- Gunata, Y. Z., Bayonove, C. L., Baumes, R. L., & Cordonnier, R. E. (1985). The aroma of grapes I. Extraction and determination of free and glycosidically bound fractions of some grape aroma components. *Journal of Chromatography A*, 331, 83–90. [https://doi.org/10.1016/0021-9673\(85\)80009-1](https://doi.org/10.1016/0021-9673(85)80009-1)
- Hjelmeland, A. K., & Ebeler, S. E. (2015). Glycosidically Bound Volatile Aroma Compounds in Grapes and Wine: A Review. *American Journal of Enology and Viticulture*, 66(1), 1. <https://doi.org/10.5344/ajev.2014.14104>
- Katarína, F., Katarína, M., Katarína, D., Ivan, Š., & Fedor, M. (2014). Influence of yeast strain on aromatic profile of Gewürztraminer wine. *LWT - Food Science and Technology*, 59(1), 256–262. <https://doi.org/10.1016/j.lwt.2014.05.057>

- Lukić, I., Radeka, S., Grozaj, N., Staver, M., & Peršurić, D. (2016). Changes in physico-chemical and volatile aroma compound composition of Gewürztraminer wine as a result of late and ice harvest. *Food Chemistry*, 196, 1048–1057. <https://doi.org/10.1016/j.foodchem.2015.10.061>
- Miyazawa, M., Yokote, K., & Kameoka, H. (1995). Biotransformation of the monoterpenoid, rose oxide, by *Aspergillus niger*. *Phytochemistry*, 39(1), 85–89. [https://doi.org/10.1016/0031-9422\(94\)00856-0](https://doi.org/10.1016/0031-9422(94)00856-0)
- Ong, P. K. C., & Acree, T. E. (1999). Similarities in the Aroma Chemistry of Gewürztraminer Variety Wines and Lychee (Litchi chinensis Sonn.). *Fruit. Journal of Agricultural and Food Chemistry*, 47(2), 665–670. <https://doi.org/10.1021/jf980452j>
- Piergiorgianni, M., Carlin, S., Lotti, C., Vrhovsek, U., & Mattivi, F. (2023). Development of a Fully Automated Method HS-SPME-GC-MS/MS for the Determination of Odor-Active Carbonyls in Wines: A “Green” Approach to Improve Robustness and Productivity in the Oenological Analytical Chemistry. *Journal of Agricultural and Food Chemistry*. <https://doi.org/10.1021/acs.jafc.2c07083>
- Plane, R. A., Mattick, L. R., & Weirs, L. D. (1980). An Acidity Index for the Taste of Wines. *American Journal of Enology and Viticulture*, 31(3), 265–268. <https://doi.org/10.5344/ajev.1980.31.3.265>
- Poulter, C. D., & King, C. H. R. (1982a). Model studies of terpene biosynthesis. A stepwise mechanism for cyclization of nerol to α -terpineol. *Journal of the American Chemical Society*, 104(5), 1422–1424. <https://doi.org/10.1021/ja00369a046>
- Poulter, C. D., & King, C. H. R. (1982b). Model studies of terpene biosynthesis. Stereospecific cyclization of N-methyl-(S)-4-([1²H]neryloxy)pyridinium methyl sulfate to α -terpineol. *Journal of the American Chemical Society*, 104(5), 1420–1422. <https://doi.org/10.1021/ja00369a045>
- Rapp, A., & Marais, J. (1993). shelf life of wine: Changes in aroma substances during storage and ageing of white wines. *Developments in Food Science*. In G. Charalambous (Ed.), *Shelf life Studies of Foods and Beverages* (pp. 891–921). Amsterdam: Elsevier.
- Sánchez-Acevedo, E., Lopez, R., & Ferreira, V. (2024). Kinetics of aroma formation from grape-derived precursors: Temperature effects and predictive potential. *Food Chemistry*, 438, Article 137935. <https://doi.org/10.1016/j.foodchem.2023.137935>
- Semikolenov, V. A., Ilyna, I. L., & Maksimovskaya, R. I. (2003). Linalool to geraniol/nerol isomerization catalyzed by (RO)3VO complexes: Studies of kinetics and mechanism. *Journal of Molecular Catalysis A: Chemical*, 204–205, 201–210. [https://doi.org/10.1016/S1381-1169\(03\)00299-1](https://doi.org/10.1016/S1381-1169(03)00299-1)
- Slaghenaufi, D., & Ugliano, M. (2018). Norisoprenoids, Sesquiterpenes and Terpenoids Content of Valpolicella Wines During Aging: Investigating Aroma Potential in Relationship to Evolution of Tobacco and Balsamic Aroma in Aged Wine. *Frontiers in Chemistry*, 6. <https://doi.org/10.3389/fchem.2018.00066>
- Timell, T. E. (1964). The acid hydrolysis of glycosides. I. general conditions and the effect of the nature of the aglycone. *Canadian Journal of Chemistry*, 42(6), 1456–1472. <https://doi.org/10.1139/v64-221>
- Ugliano, M., & Moio, L. (2008). Free and hydrolytically released volatile compounds of *Vitis vinifera* L. cv. Fiano grapes as odour-active constituents of Fiano wine. *Analytica Chimica Acta*, 621(1), 79–85. <https://doi.org/10.1016/j.aca.2008.03.002>
- Versini, G. (1985). Sull'aroma del vino 'Traminer aromatico' o 'Gewürztraminer'. *VIGNEVINI*, 12(1–2), 57–65.
- Yang, Y., Frank, S., Wei, X., Wang, X., Li, Y., Steinhaus, M., & Tao, Y. (2023). Molecular Rearrangement of Four Typical Grape Free Terpenes in the Wine Environment. *Journal of Agricultural and Food Chemistry*, 71(1), 721–728. <https://doi.org/10.1021/acs.jafc.2c07576>